IMMUNOLOGY

The regulatory subunits of PI3Kγ control distinct neutrophil responses

Arnaud Deladeriere, Laure Gambardella,* Dingxin Pan, Karen E. Anderson, Phillip T. Hawkins, Len R. Stephens†

Neutrophils, which migrate toward inflamed sites and kill pathogens by producing reactive oxygen species (ROS), are important in the defense against bacterial and fungal pathogens, but their inappropriate regulation causes various chronic inflammatory diseases. Phosphoinositide 3-kinase γ (PI3Kγ) functions downstream of proinflammatory G protein (heterotrimeric guanine nucleotide–binding protein)–coupled receptors (GPCRs) in neutrophils and is a therapeutic target. In neutrophils, PI3Kγ consists of a p110γ catalytic subunit, which is activated by the guanosine triphosphatase Ras, and either a p84 or p101 regulatory subunit. Loss or inhibition of p110γ or expression of a Ras-insensitive variant p110γ (p110γ$^{DASAA/DASAA}$) impairs PIP_3 production, Akt phosphorylation, migration, and ROS formation in response to GPCR activation. The p101 subunit binds to, and mediates PI3Kγ activation by, G protein βγ subunits, and p101$^{-/-}$ neutrophils have a similar phenotype to that of p110γ$^{-/-}$ neutrophils, except that ROS responses are normal. We found that p84$^{-/-}$ neutrophils displayed reduced GPCR-stimulated PIP_3 and Akt signaling, which was indistinguishable from that of p101$^{-/-}$ neutrophils. However, p84$^{-/-}$ neutrophils produced less ROS and exhibited normal migration in response to GPCR stimulation. These data suggest that p84-containing PI3Kγ controls GPCR-dependent ROS production. Thus, the PI3Kγ regulatory subunits enable PI3Kγ to mediate distinct neutrophil responses, which may occur by targeting PIP_3 signaling into spatially distinct domains.

INTRODUCTION

Class I phosphoinositide 3-kinases (PI3Ks) are activated by cell surface receptors to generate the signaling phospholipid phosphatidylinositol 3,4,5-trisphosphate [$PI(3,4,5)P_3$, also known as PIP_3]. This signal engages a diverse family of effector proteins, including, for example, Akt [also known as protein kinase B (PKB)], which typically contain pleckstrin homology domains and coordinate cellular responses, such as growth and movement. All of the class I PI3Ks are heterodimers composed of regulatory and catalytic subunits. There are four catalytic subunits (p110α, p110β, p110δ, and p110γ), which give their name to the relevant complex (*1*). PI3Kγ is found in many cell types, but it is most abundant in myeloid cells, particularly neutrophils (*2*). Selective inhibitors and genetic deletion of p110γ showed that it is required for G protein (heterotrimeric guanine nucleotide–binding protein)–coupled receptors (GPCRs) to stimulate PIP_3 accumulation, Akt activation, and a collection of proinflammatory responses in isolated mouse and human neutrophils, such as the formation of reactive oxygen species (ROS) and chemokinesis (increased cell movement) (*3*–*6*). PI3Kγ is required for neutrophils to accumulate at sites of inflammation in vivo (*7*).

PI3Kγ can contain one of two possible regulatory subunits: the more widely distributed p84 subunit or the relatively myeloid-specific p101 subunit (*8*, *9*). The p101 and p84 subunits are closely related to one another, but not to other proteins; they function only in complex with p110γ. GPCRs can regulate PI3Kγ through three major mechanisms. First, βγ subunits released from G proteins activate p110γ directly (*10*, *11*), but this interaction is substantially augmented through a further, probably direct, interaction between Gβγ subunits and p101 (*12*, *13*). The sensitivity of p84-PI3Kγ to activation by Gβγ is, at least, much lower than that of p101-PI3Kγ (*8*), and some reports suggest that it is insensitive (*14*). The structure and contacts within the Gβγ-activated PI3Kγ complex remain unclear. Second, p110γ contains a Ras-binding domain that enables p110γ to be activated directly by guanosine triphosphate (GTP)–bound (active) Ras (Ras-GTP) (*15*, *16*); however, Gβγ subunits and Ras-GTP activate PI3Kγ synergistically. Another study led to the hypothesis that Ras-GTP activates p84-PI3Kγ and that Gβγ subunits activate p101-PI3Kγ (*14*). In neutrophils, GPCRs increase Ras-GTP abundance through the phospholipase C-β2 and -β3 (PLC-β2/β3)–dependent, diacylglycerol (DAG)–mediated activation of RasGRP4 (Ras guanine nucleotide–releasing protein 4) (*17*). Third, in mast cells, which express only p84, the Ca^{2+}- and Akt-mediated phosphorylation of p110γ at Ser^{582} (S582) is thought to cause dissociation of p84 from p110γ and, because the regulatory subunits suppress p110γ activity, an increase in p110γ activity (*18*); however, some studies indicate that Ca^{2+} and protein kinase C (PKC) family members do not control the GPCR-stimulated accumulation of PIP_3 in neutrophils (*19*, *20*).

We previously demonstrated that mouse neutrophils expressing the variant p110γ$^{DASAA/DASAA}$, which is insensitive to activation by Ras-GTP, have a very similar, but slightly milder, phenotype than that of p110γ$^{-/-}$ neutrophils (*21*). In contrast, p101$^{-/-}$ neutrophils show reductions in the accumulation of PIP_3, activation of Akt, and cell migration in response to GPCR agonists, which are similar to those elicited by the presence of p110γ$^{DASAA/DASAA}$, but their ability to generate ROS is unchanged (*21*). These results could be explained in several ways. First, GPCR-stimulated ROS formation might be controlled only by Ras activation and not by the regulatory subunits. Second, the p84 subunit might be required for ROS formation. Third, the p84 and p101 subunits might operate redundantly, such that ROS formation depends simply on the amount of PIP_3 that is produced, regardless of its origin. This latter possibility suggests that loss of p101 might fail to reduce PIP_3 generation sufficiently to affect ROS formation and that loss of p84 might reduce ROS formation because it causes a more substantial reduction in

Signalling Department, Babraham Institute, Babraham Research Campus, Cambridge CB22 4AT, UK.
*Present address: The Anne McLaren Laboratory for Regenerative Medicine and Division of Cardiovascular Medicine, University of Cambridge, Addenbrooke's Hospital, Cambridge CB2 1QR, UK.
†Corresponding author. E-mail: len.stephens@babraham.ac.uk

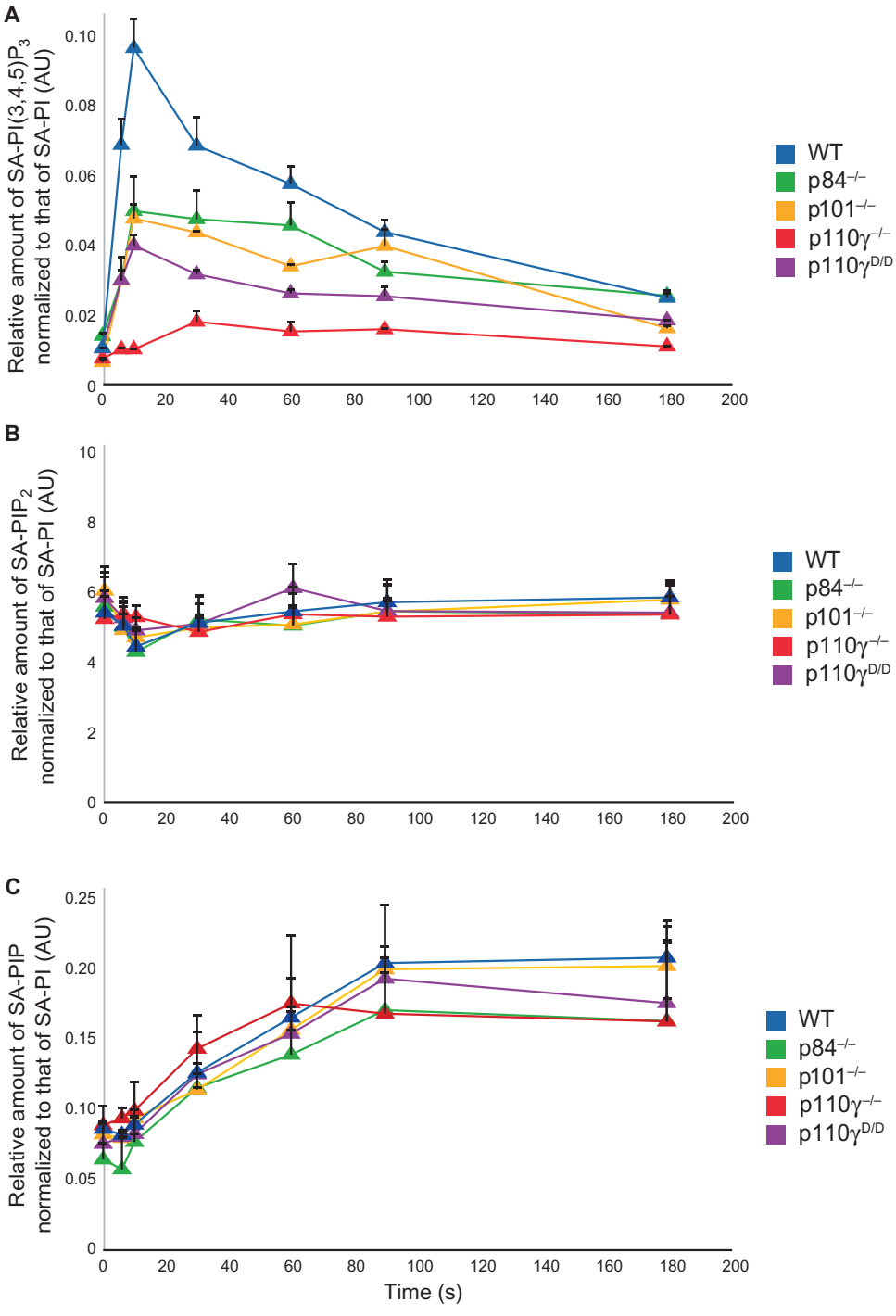

Fig. 1. Analysis of the amounts of stearoyl/arachidonoyl-PIP_3, stearoyl/arachidonoyl-PIP_2, and stearoyl/arachidonoyl-PIP in fMLP-stimulated neutrophils. (A to C) Neutrophils were left unstimulated or were stimulated for the indicated times with 10 μM fMLP and then were analyzed by mass spectrometry to determine the relative amounts of (A) SA (stearoyl/arachidonoyl)–PIP_3, (B) SA-PIP_2, and (C) SA-PIP normalized to that of SA-PI. Data are means ± SEM from 12 experiments for wild-type (WT) cells and from 3 experiments each for $p84^{-/-}$, $p101^{-/-}$, $p110\gamma^{-/-}$, and $p110\gamma^{D/D}$ cells, with every point being based on duplicate measurements in each experiment. The WT data are combined from $p84^{+/+}$ (n = 3 experiments), $p101^{+/+}$ (n = 3), and $p110\gamma^{+/+}$ (n = 6) cells. Application of a ratio-paired t test to the areas under the curve between each genotype and its corresponding WT strain gave the following P values for SA-PIP_3: $p84^{-/-}$, P = 0.0005; $p101^{-/-}$, P = 0.0084; $p110\gamma^{-/-}$, P = 0.0136; $p110\gamma^{D/D}$, P = 0.001. $p110\gamma^{D/D}$ cells were compared to $p110\gamma^{+/+}$ cells in this test. AU, arbitrary unit.

PIP_3 accumulation, or that only combined deletion of p84 and p101 might reduce PIP_3 production sufficiently to reduce the amount of ROS formed. Some, but not all, of these possibilities are consistent with the idea that Ras-GTP activates only p84-PI3Kγ. To test these possibilities, we generated and characterized a $p84^{-/-}$ mouse.

RESULTS

$p84^{-/-}$ mice are fertile, viable, and without a gross phenotype

We found that $p84^{-/-}$ mice (see Materials and Methods and fig. S1, A to C) did not have detectable p84 protein (fig. S1D), and that they were viable, fertile, and of normal size and displayed small reductions in the numbers of their circulating lymphocytes and granulocytes compared to $p84^{+/+}$ mice, but had normal red blood cell counts. There was evidence that the abundance of either p84 or p101 in neutrophils was slightly increased in the absence of the other subunit (fig. S1, D and E), suggesting that some compensation had occurred and that both subunits are found in the same cells. Note that the loci of the genes encoding p84 (*PIK3R6*) and p101 (*PIK3R5*) are within 5 kb of each other on mouse chromosome 11. Hence, the likelihood of obtaining $p84^{-/-}p101^{-/-}$ doubly deficient mice by interbreeding the two strains is extremely low and would require that the *PIK3R6* and *PIK3R5* loci on the same embryonic stem cell chromosome were appropriately targeted (work in progress).

p84 and p101 support similar amounts of PIP_3 accumulation and equivalent PI3Kγ activation in mouse neutrophils

We measured PIP_3 accumulation in bone marrow–derived neutrophils from $p84^{-/-}$, $p101^{-/-}$, $p110\gamma^{DASAA/DASAA}$, and $p110\gamma^{-/-}$ mice, as well as from their respective wild-type strains (Fig. 1). This analysis showed that, consistent with previous studies, $p110\gamma^{-/-}$ neutrophils displayed an about 95% reduction in PIP_3 accumulation in response to the GPCR

ligand formylated Met-Leu-Phe (fMLP) (*3*–*5*, *22*) compared to that in wild-type neutrophils, demonstrating the dominant role of PI3Kγ in this response. PIP_3 accumulation in response to fMLP was reduced by about 65% in p110γ$^{DASAA/DASAA}$ neutrophils and by 50% in both p84$^{-/-}$ and p101$^{-/-}$ neutrophils compared to that in wild-type cells (Fig. 1) (*21*), which suggests that p84 and p101 have similar, nonredundant roles in this response. In contrast, none of these genetic modifications had any substantial effects on the total amounts of PIP_2 (phosphatidylinositol 4,5-bisphosphate) [mostly $PI(4,5)P_2$)] or PIP (Fig. 1).

One of the most characteristic responses to PIP_3 accumulation is phosphorylation of Akt on Thr^{308} (T308, numbering based on human Akt1) by PDK-1 (3-phosphoinositide-dependent protein kinase 1) and on Ser^{473} (S473) by mammalian target of rapamycin complex 2 (mTORC2). This process represents a readout of PIP_3 abundance by a cellular effector. We measured the phosphorylation of Akt-Thr^{308} and Akt-Ser^{473} in neutrophils (which have both Akt1 and Akt2) from the above genetically modified models in response to fMLP (Fig. 2, A and B), leukotriene B_4 (LTB_4) (Fig. 3A), and C5a (fragment of complementary protein C5) (Fig. 3B); for the latter two agonists, we measured responses only in wild-type and p84$^{-/-}$ neutrophils. This analysis revealed that both phosphorylation events followed the same pattern of dependency on p84, p101, Ras-GTP, and p110γ as did PIP_3 accumulation, albeit with different kinetics. To resolve the potentially different effects of these genetic modifications on Akt1 and Akt2, we used Western blotting analysis to detect phosphorylated S473-Akt1 and S474-Akt2 This approach showed that phosphorylation of both isoforms of Akt had a similar pattern of dependency on p84, p101, and p110γ (Fig. 4). We next addressed whether loss of p84 or p101 might differentially affect the increase in cytosolic free Ca^{2+}, an important response required for activation of the neutrophil oxidase complex. We found that loss of p110γ, p84, or p101 did not substantially reduce fMLP-stimulated Ca^{2+} signaling (fig. S2, A and B).

DAG is an important intracellular signaling lipid thought to have roles in regulation of ROS formation and Ras activation through the activation of DAG sensors such as members of the PKC family or RasGRP4 (*17*). Stearoyl/arachidonoyl molecular species of DAG are thought to represent the "signaling" component of total cellular DAG that preferentially activates DAG sensors. More saturated and abundant DAG species are thought to be involved in the do novo synthesis of phospholipids. The origins and mechanisms segregating these distinct pools of DAG are not fully understood, but

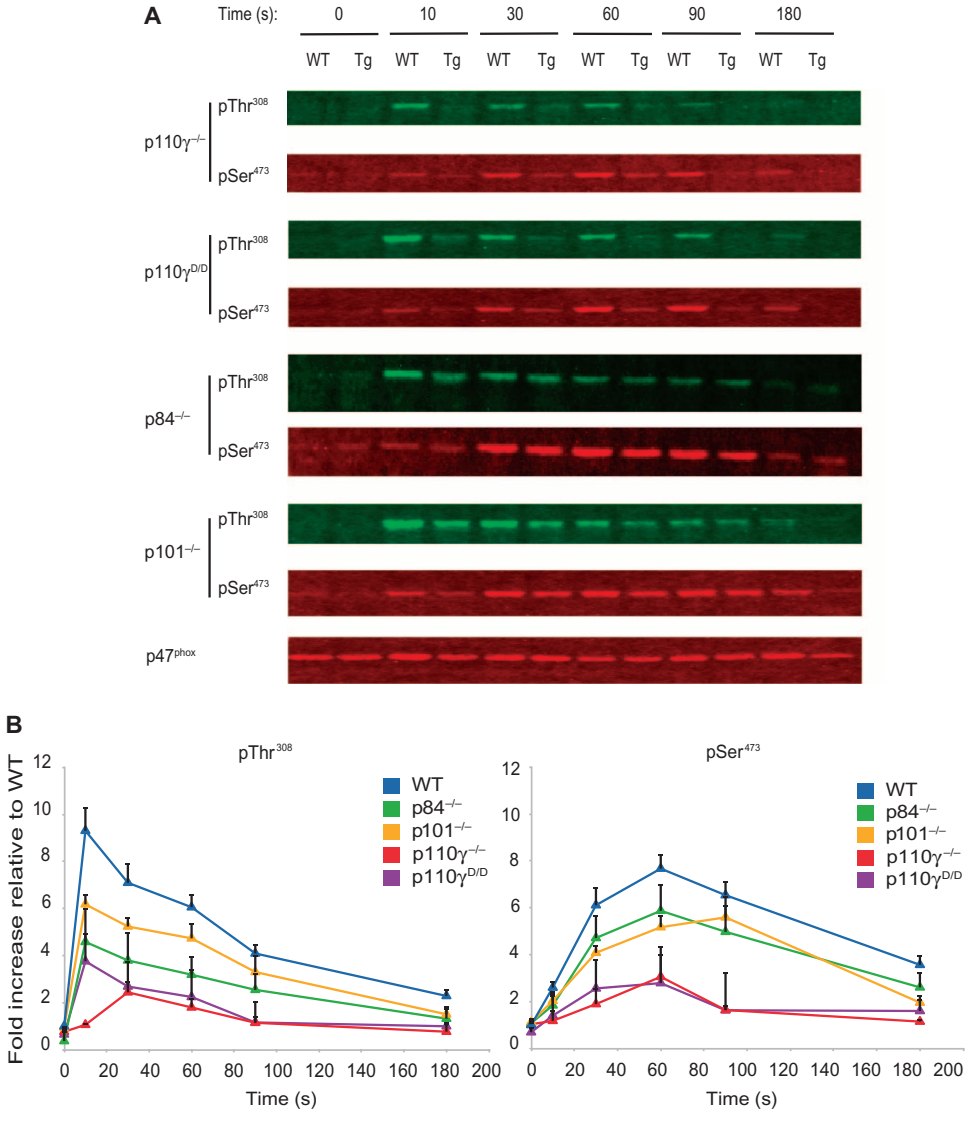

Fig. 2. Phosphorylation of Akt in response to fMLP is reduced in neutrophils from p84$^{-/-}$, p101$^{-/-}$, p110γ$^{-/-}$, and p110γ$^{D/D}$ mice. (**A**) Neutrophils isolated from p84$^{-/-}$, p101$^{-/-}$, p110γ$^{-/-}$, and p110γ$^{D/D}$ mice as well as from their corresponding WT strains were left untreated or were treated with 10 μM fMLP for the indicated times. Samples were then analyzed by Western blotting with specific antibodies to detect Akt phosphorylated at Thr^{308} (pThr^{308}) and Ser^{473} (pSer^{473}). Tg, transgenic mice. Representative Western blots are shown. (**B**) Quantification of the relative amounts of pAkt from the experiments represented in (A). Data were corrected for input material by analyzing the same membranes with antibody specific for p47^{phox} and calculating the pAkt signal/p47^{phox} signal for each sample. Data are mean fold increases in the abundance of the indicated pAkt relative to that in WT control samples ± SEM from 16 experiments for WT cells, 5 experiments for p84$^{-/-}$ and p101$^{-/-}$ mice, and 3 experiments for p110γ$^{-/-}$ and p110γ$^{D/D}$ mice, with every point in each experiment being performed in duplicate. Application of a ratio-paired *t* test to the areas under the curve between each genotype and its corresponding WT strain gave the following *P* values for Akt-pThr^{308}: p84$^{-/-}$, $P = 0.0096$; p101$^{-/-}$, $P = 0.0003$; p110γ$^{-/-}$, $P = 0.0008$; p110γ$^{D/D}$, $P = 0.0204$, and the following *P* values for Akt-pSer^{473}: p84$^{-/-}$, $P = 0.0354$; p101$^{-/-}$, $P = 0.0113$; p110γ$^{-/-}$, $P = 0.0073$; p110γ$^{D/D}$, $P = 0.0256$. p110γ$^{D/D}$ cells were compared to p110γ$^{+/+}$ cells in this test.

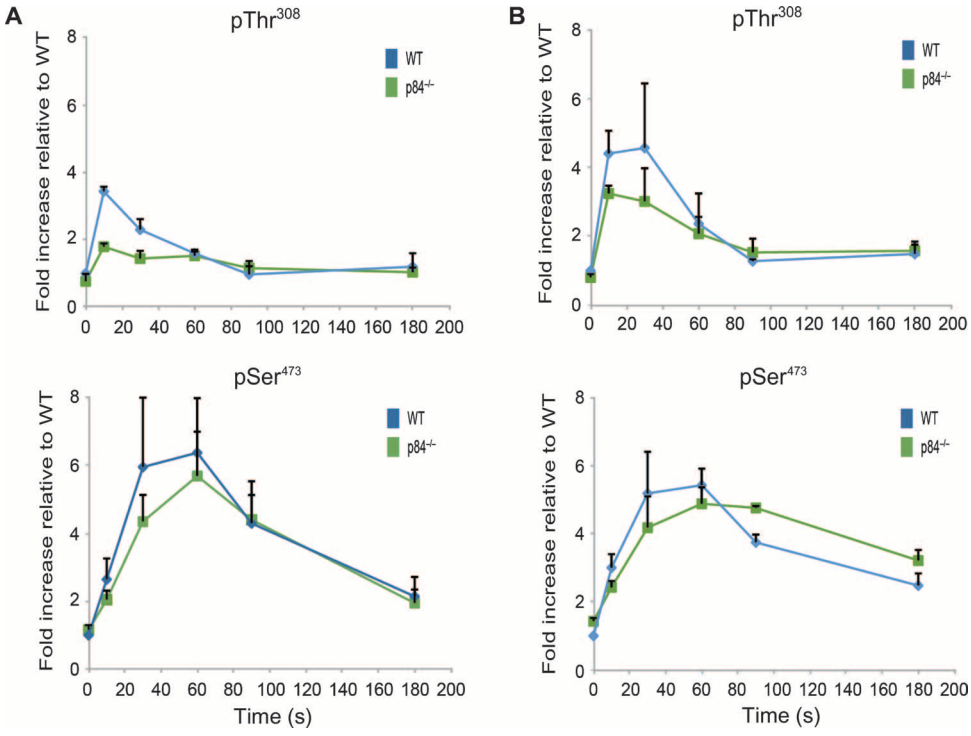

Fig. 3. Phosphorylation of Akt in response to chemoattractants is reduced in neutrophils from p84$^{-/-}$ mice. (A and B) Neutrophils isolated from WT and p84$^{-/-}$ mice were left untreated or were treated with (A) 100 nM C5a or (B) 100 nM LTB_4 for the indicated times. Samples were then analyzed by Western blotting, and the relative amounts of Akt-pThr^{308} and Akt-pSer^{473} were determined as described for Fig. 2. Data are means ± SD from three independent experiments, each performed in duplicate. The extent of phosphorylation of Akt at Thr^{308} after 10 s of stimulation with either C5a or LTB_4 was statistically significantly lower in p84$^{-/-}$ neutrophils than in WT neutrophils (P = 0.02 for C5a and P = 0.04 for LTB_4, by t test).

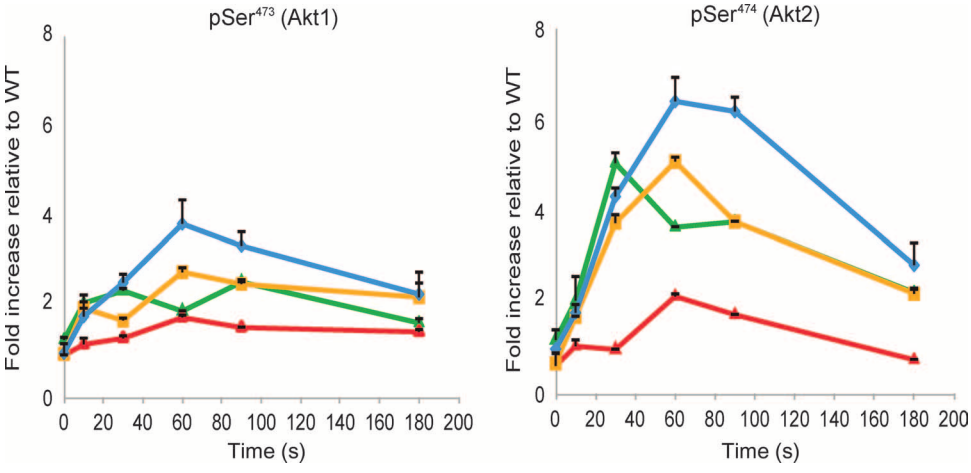

Fig. 4. Phosphorylation of Ser^{473} (Akt1) and Ser^{474} (Akt2) in fMLP-stimulated neutrophils. Neutrophils isolated from p84$^{-/-}$, p101$^{-/-}$, and p110γ$^{-/-}$ mice, as well as from their corresponding WT strains, were left untreated or were treated with 10 μM fMLP for the indicated times. Samples were then analyzed by Western blotting, and the relative amounts of Akt1-pSer^{473} (left) and Akt2-pSer^{474} (right) were determined as described for Fig. 2. Data are means ± SEM from nine experiments for WT cells and from three experiments each for p84$^{-/-}$, p101$^{-/-}$, and p110γ$^{-/-}$ cells. Application of a ratio-paired t test to the areas under the curve between each genotype and its corresponding WT stain gave the following P values for p110γ$^{-/-}$: Akt1, P = 0.036; Akt2, P = 0.015.

an important feature is that the phosphoinositide substrates of PLCs are enriched in stearoyl/arachidonoyl species; hence, PLC activity generates DAG enriched in those species (*23*). This means that stearoyl/arachidonoyl-DAG, and not total DAG, is the best measure of cellular PLC activity and the likely activation of DAG sensors. Hence, we addressed the question of whether PI3Kγ signaling regulates stearoyl/arachidonoyl-DAG formation as a precursor to considering the possibility that p84-PI3Kγ and p101-PI3Kγ might differentially control neutrophil responses through their ability to selectively control stearoyl/arachidonoyl-DAG accumulation. We found that loss of p110γ had no marked effect on fMLP-stimulated stearoyl/arachidonoyl-DAG production (fig. S2C). Given that the phenotypes resulting from loss of p84 or p101 are very likely to be a part of the p110γ$^{-/-}$ phenotype, we assumed it unlikely that p84 and p101 might differentially control stearoyl/arachidonoyl-DAG production.

These data support the notion that p84- and p101-containing PI3Kγ complexes support PIP_3 accumulation, PI3Kγ activation, and Akt activation to similar extents. Furthermore, other important intracellular signals did not appear to be differentially regulated by the PI3Kγ regulatory subunits. These data also showed that p84, similar to p101, p110γ, and the Ras-dependent activation of PI3Kγ, functions downstream of a number of GPCRs on neutrophils and not just fMLP receptors.

In contrast to p101, p84 has no role in the regulation of neutrophil migration either in vitro or in vivo

Mouse neutrophils accumulate in the peritoneum after mice are injected with sterile chemical irritants, and previous studies showed that p110γ and the Ras-dependent activation of p110γ and p101 are required for this process (*3–5*, *21*). We measured the accumulation of neutrophils in the peritoneum after thioglycollate was injected into p84$^{-/-}$ and p101$^{-/-}$ mice and their respective wild-type controls. We found that the accumulation of neutrophils in the peritoneum was substantially reduced in p101$^{-/-}$ mice compared to that in wild-type controls, consistent with previous work (*21*), but not in p84$^{-/-}$ mice (Fig. 5A). A previous study indicated that the accumulation of neutrophils in an inflamed peritoneum requires p110γ to be present in bone marrow cells and endothelial cells (*24*). We therefore investigated whether this apparent lack of a role for

Fig. 5. The migration of neutrophils in vivo depends on p101, but not p84. (A) Thioglycollate was injected into the peritoneums of mice of the indicated genotypes. As a negative control, some of the indicated mice were not injected. After 4.5 hours, the neutrophils that accumulated in the peritoneums of the injected and control mice were collected and quantified. Data are expressed as a percentage of the number of cells that accumulated in the peritoneums of thioglycollate-injected WT mice. Data are means ± SEM from four experiments for $p84^{-/-}$ mice, representing 16 mice each for WT and $p84^{-/-}$, and from four experiments for $p101^{-/-}$ mice, representing 15 mice each for WT and $p101^{-/-}$. Application of a ratio-paired *t* test to compare between each genotype and its corresponding WT stain gave the following *P* values: $p84^{-/-}$, $P = 0.3906$; $p101^{-/-}$, $P = 0.0047$. (**B**) Lethally irradiated WT mice that had been reconstituted with bone marrow (BM) cells from WT, $p84^{-/-}$, or $p101^{-/-}$ mice, as indicated, were left uninjected or were injected with thioglycollate, and the numbers of neutrophils that accumulated in the peritoneum were determined as described in (A). Data are means ± SEM from three experiments representing 12 mice for each of the backgrounds. Application of a ratio-paired *t* test gave the following *P* values: $p84^{-/-}$ cells into WT, $P = 0.5963$; $p101^{-/-}$ cells into WT, $P = 0.0016$. (**C**) Bone marrow cells (1×10^6) from mice of the indicated genotype were loaded into the upper chamber of a Transwell insert. Control buffer or 1 μM fMLP was placed in the lower chamber. Migration was assessed by counting the numbers of neutrophils that appeared in the lower chamber after 1 hour of incubation. Data are expressed as a percentage of the number of WT neutrophils that migrated to fMLP. Data are means ± SEM from four experiments for each genotype. Application of a ratio-paired *t* test to compare each genotype with its corresponding WT strain gave the following *P* values: $p84^{-/-}$, $P = 0.7937$; $p101^{-/-}$, $P = 0.0219$; $p110\gamma^{-/-}$, $P = 0.0383$. $^*P < 0.05$; $^{**}P < 0.01$.

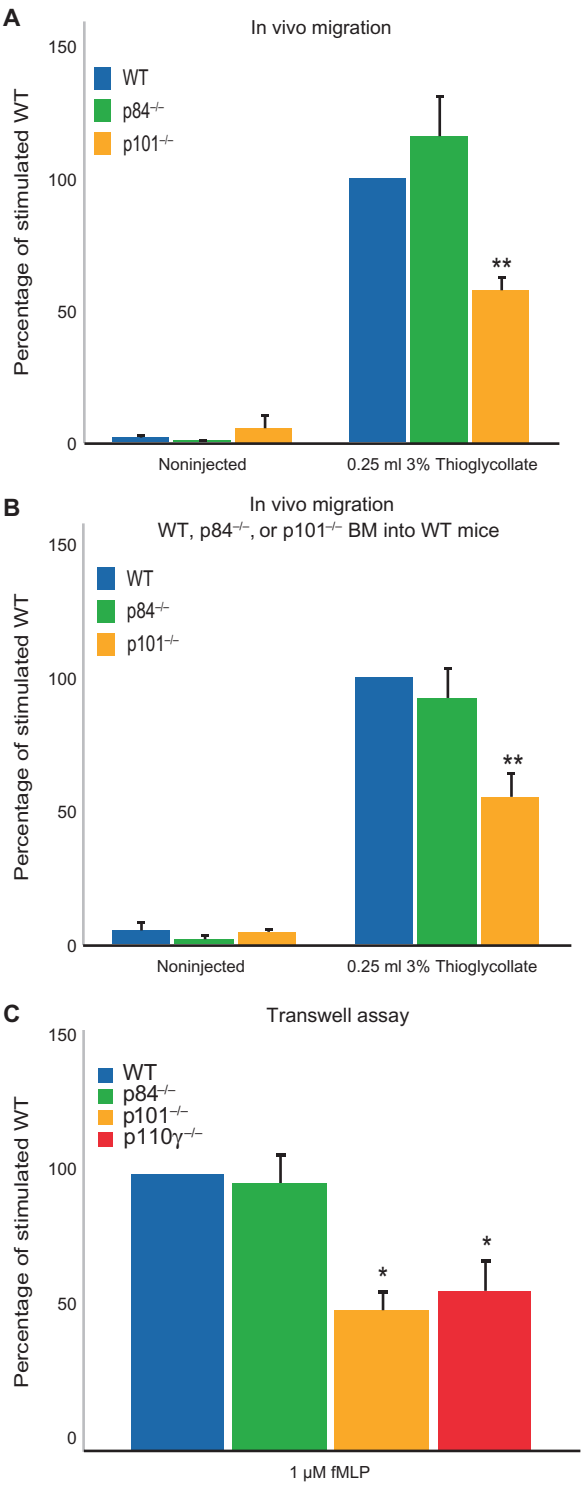

p84 in neutrophil accumulation during peritonitis was because an underlying role in bone marrow cells was masked by compensating roles for p84 in other tissues that normally suppress the response. To do this, we generated bone marrow chimeric mice by transferring stem cells from $p84^{-/-}$ or $p101^{-/-}$ mice or their wild-type controls into irradiated recipient $p84^{-/-}$, $p101^{-/-}$, or wild-type control mice. We found that loss of p101, but not p84, in the bone marrow cells alone, reduced neutrophil accumulation in the peritoneum (Fig. 5B).

To further refine these observations, we measured the movement of isolated neutrophils in two in vitro assays of migration. First, we used Transwell filter assays, which measure chemokinesis and have been used to show that $p110\gamma^{-/-}$, $p101^{-/-}$, and $p110\gamma^{DASAA/DASAA}$ neutrophils have reduced chemokinetic responses to chemoattractants compared to those of wild-type neutrophils (*6*, *21*). Second, we used microscopic observation chambers with stable gradients of chemoattractants, which enabled us to measure individual cell tracks and therefore the chemotactic efficiency of migration. This latter assay has been used to demonstrate that p110γ is required for chemokinesis, but not for normal gradient-sensing or chemotactic efficiency (*6*, *25*). We found that $p101^{-/-}$, $p110\gamma^{-/-}$, and $p110\gamma^{DASAA/DASAA}$ neutrophils, but not $p84^{-/-}$ neutrophils, had reduced chemokinetic responses in both assays (Figs. 5C and 6A) (*21*). Consistent with previous work (*6*), the absence of p110γ had no effect on chemotactic efficiency, and furthermore, nor did the absence of p84 or p101 or the expression of a Ras-insensitive variant of p110γ (Fig. 6B). These types of PI3Kγ-sensitive defects in chemokinesis are associated with, and are thought to be caused by, reductions in the speed and extent of chemoattractant-induced polarization of polymerized actin (F-actin) (*6*). Consistent with this, $p110\gamma^{-/-}$ neutrophils exhibit less efficient polarization of their F-actin in response to chemoattractants than do wild-type neutrophils. We measured the polarization of F-actin in control and chemoattractant-stimulated $p84^{-/-}$, $p101^{-/-}$, $p110\gamma^{-/-}$, and wild-type neutrophils and found that it was substantially reduced in $p101^{-/-}$ and $p110\gamma^{-/-}$, but not $p84^{-/-}$, neutrophils (Fig. 6C). Collectively, these results suggest that p101 has a distinct, nonredundant role in PI3Kγ-dependent chemokinesis and cytoskeletal rearrangement.

Fig. 6. Migration of neutrophils in vitro and polarization of F-actin depend on p101, but not p84. (A) Neutrophils from mice of the indicated genotypes were loaded on one side of an EZ-TAXIScan chamber, with 30 μM fMLP on the other side. Migration was assessed by counting the number of neutrophils that had moved a total accumulated distance of more than 25 μm. Data are expressed as percentages of the numbers of WT cells that migrated. Data are means ± SEM from four experiments for each genotype. Application of a ratio-paired *t* test to compare between each genotype and its corresponding WT strain gave the following *P* values: $p84^{-/-}$, *P* = 0.7168; $p101^{-/-}$, *P* = 0.0369; $p110\gamma^{-/-}$, *P* = 0.0267; $p110\gamma^{D/D}$, *P* = 0.0295. (B) The individual tracks of neutrophils from the experiments presented in (A) were analyzed to measure their migratory index: the distance from the origin/the total distance travelled. None of the migratory indexes were statistically significantly different from that of the WT control cells: *P* = 0.65, 0.13, 0.81, and 0.76 for $p84^{-/-}$, $p101^{-/-}$, $p110\gamma^{-/-}$, and $p110\gamma^{DASAA/DASAA}$ cells, respectively. (C) Neutrophils isolated from mice of the indicated genotypes were left unstimulated or were stimulated with 5 μM fMLP for 1 min before F-actin was labeled with TRITC (tetramethyl rhodamine isothiocyanate)–phalloidin. Data are expressed as a percentage of the number of WT cells that had polymerized F-actin. Data are means ± SEM from three experiments for each genotype and represent a total of at least 400 cells each. Application of a ratio-paired *t* test to compare each genotype with its corresponding WT strain gave the following *P* values: $p84^{-/-}$, *P* = 0.8305; $p101^{-/-}$, *P* = 0.0051; $p110\gamma^{-/-}$, *P* = 0.0132. *$P < 0.05$; **$P < 0.01$.

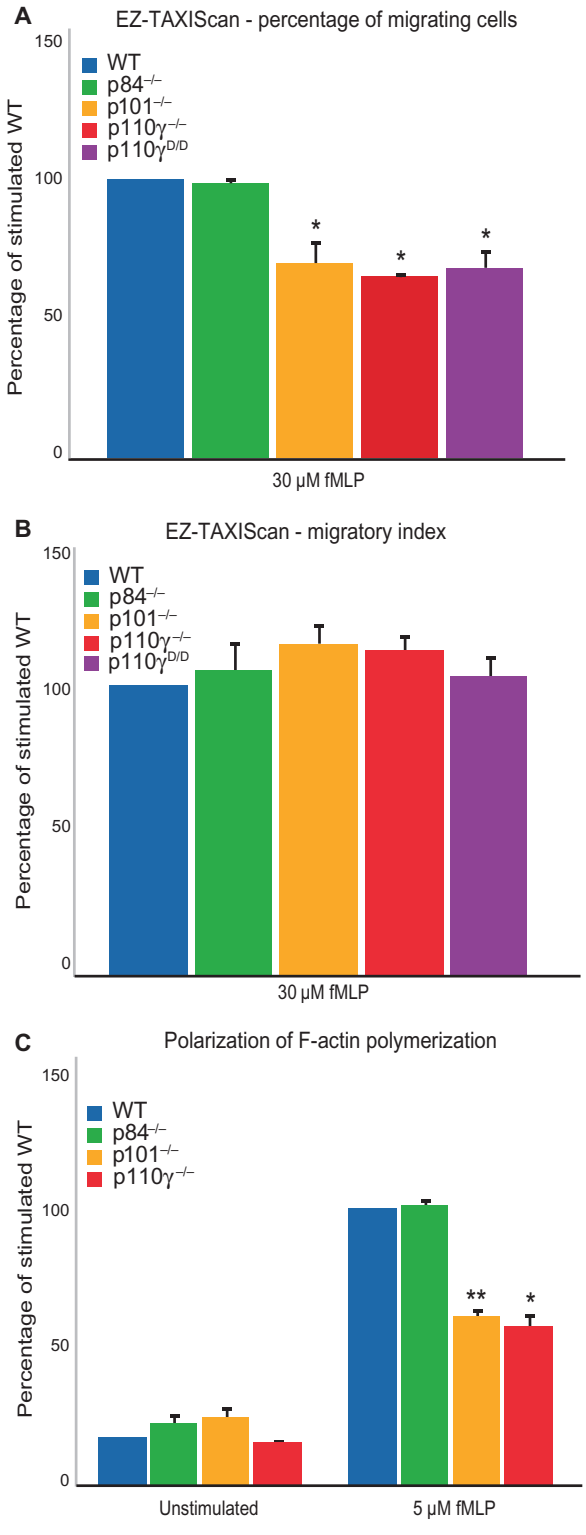

p84, but not p101, has an important role in chemoattractant-stimulated ROS formation

Chemoattractants stimulate isolated neutrophils to produce a burst of ROS that is substantially diminished in the absence of p110γ (*3*–*5*) or in cells expressing $p110\gamma^{DASAA/DASAA}$ but is unchanged by the absence of p101 (*21*). We measured ROS production in neutrophils stimulated by fMLP, LTB_4, C5a, or the phorbol ester phorbol 12-myristate 13-acetate (PMA). The results showed that loss of p84 or p110γ or expression of $p110\gamma^{DASAA/DASAA}$, but not loss of p101, reduced ROS formation to a range of submaximal concentrations of fMLP (Fig. 7, A and B). Furthermore, $p84^{-/-}$ neutrophils produced less ROS in response to C5a and LTB_4 than did wild-type neutrophils (Fig. 7, C and D), whereas their ability to produce ROS in response to phorbol esters was unchanged (Fig. 7E). These results suggest that the loss of p84 did not reduce the capacity of the neutrophils to produce ROS, that p84 functions downstream of a number of GPCRs on neutrophils, and that p84 has distinct, nonredundant roles in the GPCR-dependent regulation of ROS formation. Although the absence of p101 had no effect on the peak ROS response to fMLP, it seemed to slow the kinetics of the response slightly without substantially reducing the total amount of ROS formed over time (Fig. 7B). Perhaps this was a consequence of the small increase in p84 abundance in neutrophils in the absence of p101, which highlights the potential risks of overexpressing PI3Kγ subunits.

DISCUSSION

Thus far, there have been no genetic studies of the physiological or pathological functions of the endogenous p84 subunit; however, several studies identified roles for p84. A role for p84, but not p101, in mast cell secretory responses was defined by heterologously expressing p84, p101, or p110γ in cultured primary $p110\gamma^{-/-}$ mouse mast cells (*26*). Because p101 is not found in mast cells, the relevance of this apparent selectivity for p84 is not clear. Some evidence indicates that p84 can associate more strongly than an equivalent p101 construct with heterologously expressed phosphodiesterase-3B (PDE-3B) in human embryonic kidney cells (*9*), suggesting that p84 may have a role in the PI3Kγ-mediated regulation of PDE and myocardial contractility (*27*). Finally, in contrast to p101, p84 suppresses the growth of breast cancer–derived cell lines (*28*). Because nontransformed human breast epithelial cells do not have any PI3Kγ subunits, this finding may only be a pathophysiologically relevant observation.

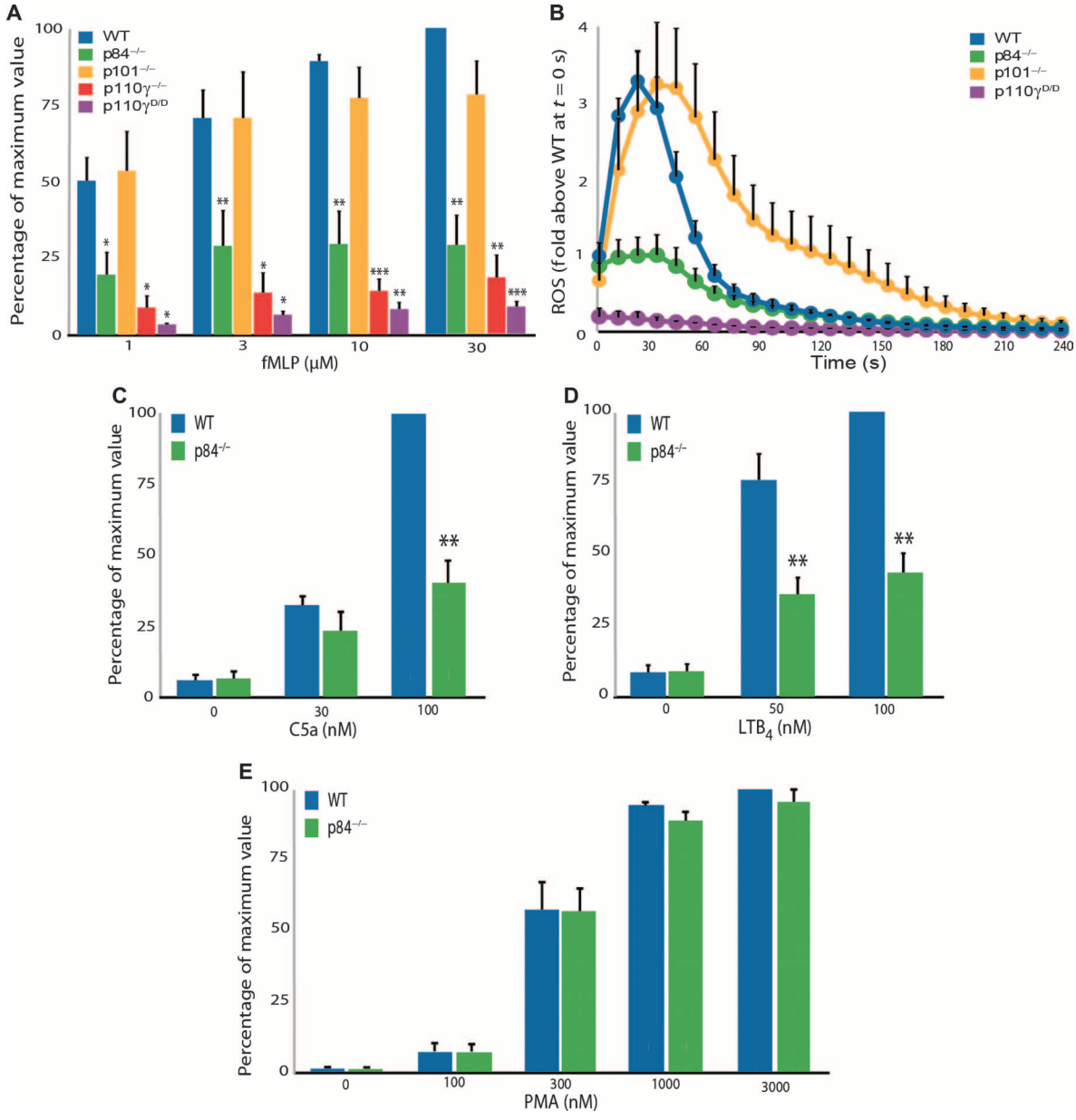

Fig. 7. The p110γ-dependent production of ROS by mouse neutrophils is dependent on p84, but not p101. (**A**) Unprimed neutrophils isolated from p84$^{-/-}$, p101$^{-/-}$, p110γ$^{-/-}$, and p110γ$^{D/D}$ mice, as well as from their corresponding WT strains, were stimulated with the indicated concentrations of fMLP, and the amounts of ROS produced were quantified by chemiluminescence assay. WT represents an average of the response of neutrophils isolated from p84$^{+/+}$, p101$^{+/+}$, and p110γ$^{+/+}$ mice. Data are expressed as percentages of the response of neutrophils isolated from WT mice. Data are means ± SEM from six experiments for WT cells; four experiments each for p84$^{-/-}$, p101$^{-/-}$, and p110γ$^{-/-}$ cells; and three experiments for p110γ$^{D/D}$ cells. Application of a ratio-paired *t* test to compare each genotype to its corresponding WT strain gave the following *P* values: p84: 30 μM, P = 0.006; 10 μM, P = 0.004; 3 μM, P = 0.022; 1 μM, P = 0.026; p101: 30 μM, P = 0.149; 10 μM, P = 0.257; 3 μM, P = 0.552; 1 μM, P = 0.815; p110γ$^{-/-}$: 30 μM, P = 0.002; 10 μM, P = 0.0005; 3 μM, P = 0.006; 1 μM, P = 0.021; and p110γ$^{D/D}$: 30 μM, P = 0.0006; 10 μM, P = 0.002; 3 μM, P = 0.052; 1 μM, P = 0.051. The difference between p84$^{-/-}$ neutrophils and either p110γ$^{-/-}$ or p110γ$^{D/D}$ neutrophils was statistically significantly different (p110γ$^{-/-}$, P = 0.002; p110γ$^{D/D}$, P = 0.003). (**B**) The rate of ROS formation by unprimed neutrophils isolated from p84$^{-/-}$ and p101$^{-/-}$ mice, as well as from their respective WT strains, was measured in the same experiments presented in (A). Data are expressed as the fold increase in ROS production compared to that of WT neutrophils at *t* = 0 s. Data are means ± SEM from five experiments for WT cells, four experiments each for p84$^{-/-}$ and p101$^{-/-}$ cells, and three experiments for p110γ$^{D/D}$ cells. (**C** to **E**) Unprimed neutrophils isolated from WT (p84$^{+/+}$) and p84$^{-/-}$ mice were stimulated with the indicated concentrations of (C) C5a, (D) LTB_4, and (E) PMA, and the amounts of ROS produced were quantified by chemiluminescence assay. Data are expressed as percentages of the response of neutrophils isolated from WT mice. Data are means ± SEM from five experiments each for C5a and PMA and four experiments for LTB_4. Application of a ratio-paired *t* test gave the following *P* values: C5a: 100 nM, P = 0.002; 30 nM, P = 0.272; LTB_4: 100 nM, P = 0.006; 50 nM, P = 0.01. *P < 0.05; **P < 0.01; ***P < 0.001.

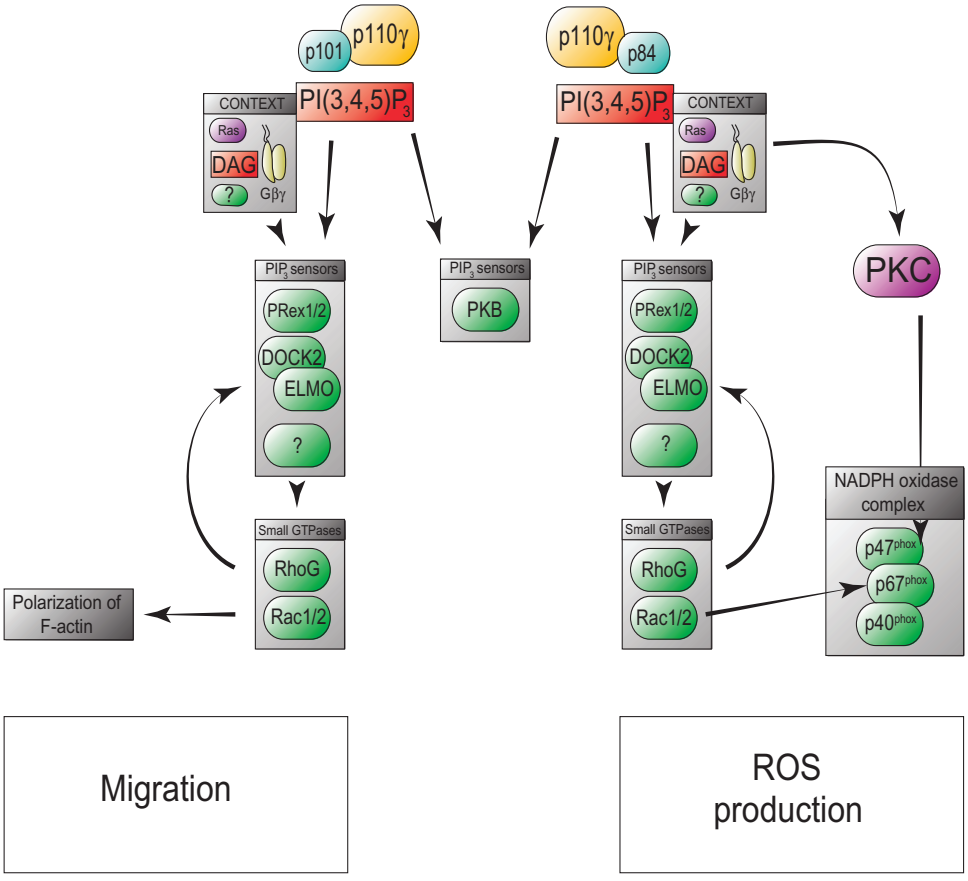

Fig. 8. Proposed model of PI3Kγ-dependent neutrophil functions. After activation of a neutrophil GPCR, a number of intracellular signals, in the forms of relevant changes in Ras, DAG, Gβγ, and PIP_3, are elicited. These factors engage further signaling that leads to the emergence of ROS and migratory responses. p84-containing PI3Kγ complexes generate PIP_3 in the context of other relevant signals, which is crucial for the formation of ROS. p101-containing PI3Kγ complexes generate PIP_3 in the context of a distinct set of relevant signals, which are important for migration. NADPH, reduced form of nicotinamide adenine dinucleotide phosphate.

Mouse neutrophils have both p84 and p101. Our results suggest that these subunits contribute almost equivalently to the production of PIP_3 and the phosphorylation of Akt, but differentially to specific cell responses. Because there was some increase in the abundance of one subunit when the other subunit was lost, it is possible that our results represent underestimates of the true dependencies on p84 and p101. This question will be partially clarified with the availability of a $p101^{-/-}p84^{-/-}$ doubly deficient mouse.

Our results suggest that p84 has distinct physiological roles in neutrophils, which cannot be supported by p101 (or indeed, by marginally increased amounts of p101), in the pathway by which GPCRs control ROS formation. This role is entirely consistent with the known roles of p110γ, and it is likely that the effect of loss of p84 on ROS formation is because of its effects on PIP_3 accumulation in response to GPCRs. The identities of the PIP_3-binding proteins that regulate the neutrophil oxidase complex after G protein activation remain unclear. The guanine nucleotide exchange factors PRex1 and PRex2 and DOCK2 (dedicator of cytokinesis 2) and the small guanosine triphosphatases (GTPases) RhoG, Rac1, and Rac2 are involved (*29*), but the scale of the role of Akt, possibly through the direct phosphorylation of $p47^{phox}$ (47-kD protein component of the phagocyte oxidase that generates ROS) or other PIP_3 sensors, is unresolved.

These results rule out two of the three potential mechanisms that could explain the PI3Kγ-dependent regulation of ROS formation (see Introduction), and show that p84 and Ras activation and binding to p110γ, but not p101, are required. Forming this conclusion appears to support the idea that Ras-GTP activates only p84-PI3Kγ. However, the discrepancies between the phenotype of $p110\gamma^{DASAA/DASAA}$-expressing neutrophils and that of $p84^{-/-}$ neutrophils suggest that this is an oversimplification. The simplest explanation we can see for these observations is that only those molecules of PI3Kγ that contain p84 and that are activated by Ras-GTP provide the appropriate signal to control ROS formation, although Ras-GTP can also activate p101-PI3Kγ. This suggests that it is the PIP_3 that is generated by the form of PI3Kγ that is activated by Ras-GTP and contains p84 that is crucial, and that the PIP_3 generated by other PI3Kγ complexes, even if similar in abundance, is less important. This would imply that stringent signal filtering is in operation. Given the known properties of the PIP_3 signaling system, it seems reasonable to speculate that it is the location of the PIP_3 that is key.

There are a number of PIP_3-independent signals that are required in the pathway by which GPCRs control ROS production, such as the PLC-β2/β3–dependent activation of Ca^{2+}, DAG, and PKC signaling. These additional signals have their own spatiotemporal dynamics that must have physical overlap with each other and relevant PIP_3 signals to enable them to combine to control ROS formation. The activation of Ras in neutrophils is stimulated by the PLC-β2/β3–stimulated generation of DAG. Thus, one could argue that the relevant part of the total Ras-GTP signal is generated within a similar spatial signaling domain to that in which the ROS-relevant DAG and PKC signals are formed. This suggests that spatially defined coincidence detection is built into this cascade. This form of filtering could ensure that PIP_3 generated by other PI3Kγ complexes that are subject to other distinct patterns of regulation, and that might regulate other cell responses, would not affect ROS formation.

We do not know the nature of these proposed spatially restricted signaling domains, containing Ras-GTP-p84-PI3Kγ and perhaps PKCs, which are key regulators of ROS formation by GPCRs. Work over the last decade has begun to reveal that Ras-GTP signaling can be concentrated into nanodomains in the plasma membrane (and other membranes) of 10 to 80 nm in scale that are very dynamic and transient in nature and are held together by large numbers of low-affinity lipid-protein, lipid-lipid, and protein-protein interactions (*30*). We would argue that these types of domains could potentially explain our findings. It would not be possible to visualize these types of domain with current fluorescent PIP_3 or DAG reporters through

standard confocal fluorescence microscopy; however, there was a report that in cultured, transfected mouse mast cells, a PIP_3 sensor showed a difference in distribution when the cells were forced to express p101 as compared to p84 (*26*).

This compartmentalized view of PI3Kγ signaling suggests that domains are assembled (or may self-assemble) that help to orchestrate the coincident signals required to engage specific cell responses. Hence, although PIP_3 is only one of the key signals, it is likely to be part of the domains that control ROS formation. PIP_3 probably accumulates in these regions because it is generated by p84-containing PI3Kγ molecules that have been recruited to those sites by their regulators and Ras-GTP. We propose that this PIP_3 is then detected by PIP_3 sensors and effectors (including PRex1, PRex2, DOCK2, RhoG, Rac1, and Rac2) that can only work productively when present together in the correct context to enable activation of the neutrophil oxidase complex (Fig. 8). In conclusion, our findings, together with those of others, suggest that p84, p101, and Ras function with other components of GPCR signaling pathways in neutrophils to enable apparently common signals to be filtered and resolved into a potentially rich repertoire of discrete, cell response–tuned codes.

MATERIALS AND METHODS

Mice

A targeting vector for p84 (which is encoded by *PIK3R6*) had already been generated by the European Conditional Mouse Mutagenesis Program (EUCOMM) project and was provided by W. C. Skarnes (from the Wellcome Trust Sanger Institute, UK) (*31*). The targeting vector consisted of two homology arms, the 5′ arm comprising exon 3 and the 3′ arm comprising exons 5 to 8 (fig. S1A). Exon 4 was flanked by two *loxP* sequences, and its removal from the genome would generate a shift in the open reading frame after splicing and an early termination of translation. The remaining peptide, of limited length, does not contain any known important domain and is likely to be degraded. The selection cassette was a promoterless neomycin resistance cassette, enabling the endogenous promoter to drive the expression of the resistance gene. The promoterless selection cassette present in the EUCOMM vector was replaced by two elements present in pACN (*32*): a neomycin resistance gene under the control of a PGK (phosphoglycerate kinase) promoter and a self-excising Cre recombinase cassette under the control of a testis-specific angiotensin-converting enzyme (tACE) promoter. Because both elements are flanked by *loxP* sites (fig. S1A), this construct enabled the cassette to be deleted in the testis of the male chimeras, giving spontaneously heterozygous $p84^{+/-}$ germline cells (fig. S1B). The 5′ and 3′ probes were amplified by polymerase chain reaction (PCR) with the primers 5′ probe forward, 5′ probe reverse, 3′ probe forward, and 3′ probe reverse (table S1), and they were used to detect a 13-kb Bam HI fragment for the wild-type allele (fig. S1B). For the targeted allele, a 6.4-kb Bam HI fragment was detected with the 5′ probe, and a 7.2-kb Bam HI fragment was detected with the 3′ probe. An internal probe, NeoP, was used to assess the number of copies of the targeting vector that had been incorporated into the genome. This probe was amplified by PCR with the primers NeoP forward and NeoP reverse (table S1). In the case of a correct single insertion of the vector, a 1.6-kb fragment was detectable with the NeoP probe (fig. S1B). Two of 10 cell clones, BH12 and BD9 (fig. S1B), were chosen to be expanded and injected into $C57BL/6J\text{-}Tyr^{C\text{-}2J}$ ("white C57BL/6J") embryos (fig. S1B) by the Gene Targeting Facility at the Babraham Institute. The $p84^{-/-}$ mice were viable and of normal size with normal blood counts (Fig. 1C). We used this first generation of $p84^{-/-}$ mice and their $p84^{+/+}$ littermates to set up breeding pairs and provide us with sufficient $p84^{-/-}$ and $p84^{+/+}$ mice. The $p84^{-/-}$ mice were fertile and born at the expected Mendelian ratio. The $p110\gamma^{-/-}$ (*3*), $p101^{-/-}$ (*21*), and $p110\gamma^{DASAA/DASAA}$ (*21*) mouse strains were described previously. For each experiment, wild-type mice that were closely related to the experimental strain were used as controls, unless otherwise stated. All mice used in further experiments were between 8 and 12 weeks of age, unless stated otherwise. Mouse strains were all housed in the Babraham small animal unit at the Babraham Institute and were kept under specified pathogen–free conditions. A PCR-based genotyping strategy using the primers listed in table S1 was implemented to manage the breeding of the different strains.

Purification of primary mouse neutrophils for ROS, Akt, and PIP_3 assays

To purify neutrophils from bone marrow, a discontinuous gradient of Percoll (GE Healthcare) was used. A 90% stock was made with 1× HBSS (Hanks' balanced salt solution) made from 10× HBSS (Gibco, Life Technologies). The 1× HBSS was supplemented with $NaHCO_3$ (3.5 g/liter, Sigma).

Mice were culled by increasing concentrations of CO_2 and cervical dislocation, and the hind femurs and tibias were removed and collected. Once the muscle and the distal ends of the bones were removed, the bone marrow was collected with a 21-gauge needle into HBSS without Ca^{2+} and Mg^{2+} (Sigma) supplemented with 15 mM Hepes (1 M Hepes, endotoxin-free, Sigma), 0.5% fatty acid–free bovine serum albumin (BSA, Sigma), and 64 ml of doubly distilled water (ddH_2O) (Gibco) per liter of solution; this buffer will be called Wash Buffer. The bone marrow cells were then resuspended in Wash Buffer, and any clumps were allowed to resettle. The suspension of cells was then centrifuged once at 500*g* in Wash Buffer, resuspended in 3 ml of Wash Buffer, and loaded onto a Percoll gradient (4 ml of 55% Percoll overlaid on 6 ml of 62% Percoll) and centrifuged at 1400*g* at room temperature for 30 min. The cells at the interface were harvested and centrifuged at 500*g* in Wash Buffer at room temperature. The cells were then resuspended in 5 ml of Gey's solution, which is a 7:2:0.5:0.5 mixture of ddH_2O, Gey's A (130 mM NH_4Cl, 5 mM KCl, 0.8 mM Na_2HPO_4, 0.176 mM KH_2PO_4, and 5.56 mM glucose), Gey's B (1.035 mM $MgCl_2\text{-}6H_2O$, 0.284 mM $MgSO_4\text{-}7H_2O$, and 1.53 mM $CaCl_2\text{-}2H_2O$), and Gey's C (13.39 mM $NaHCO_3$) for 5 min to eliminate red blood cells. The suspension was then washed three more times. Cell purity was assessed by flow cytometry (forward scatter and side scatter only) and was typically between 60 and 80%. The total number of cells was counted on a hemocytometer, and the final concentration of cells in Dulbecco's phosphate-buffered saline (dPBS, Sigma) containing Ca^{2+} and Mg^{2+} ($dPBS^{++}$) supplemented with 0.03% $NaHCO_3$ (Sigma) and 0.1% glucose (Sigma) was adjusted depending on the assay.

Purification of mouse neutrophils for in vitro EZ-TAXIS assays, Transwell assays, and measurement of F-actin polymerization

Mice were culled, and the femurs and tibias were removed and collected in ice-cold Wash Buffer as described earlier. The bone marrow was collected with a 21-gauge needle into ice-cold Wash Buffer and then resuspended, and the clumps were allowed to settle. The suspension of cells was then centrifuged once at 500*g* in ice-cold Wash Buffer, resuspended in 20 ml of ice-cold Wash Buffer, loaded onto 10 ml of ice-cold 55% Percoll, and centrifuged at 1400*g* at 4°C for 30 min. The cells at the surface of the Percoll phase were discarded, and the cell suspension was centrifuged at 500*g* in Wash Buffer at 4°C. The cells were then resuspended in 5 ml of ice-cold Gey's solution for 5 min to eliminate red blood cells. The suspension was then washed once more in ice-cold Wash Buffer. Neutrophil purity was assessed by flow cytometry and was typically between 35 and

45%. The total number of cells was counted on a hemocytometer, and the final concentration of cells in ice-cold dPBS^{++}, 0.25% BSA, 15 mM Hepes (supplemented with $NaHCO_3$ and glucose) was adjusted to 3×10^5 neutrophils/ml.

Western blotting analysis

SDS–polyacrylamide gel electrophoresis (SDS-PAGE) gels were made with separating buffer [750 mM tris (pH 8.8), 0.2% SDS] and stacking buffer [250 mM tris (pH 6.8), 0.2% SDS], acrylamide (Bio-Rad), ammonium persulfate, and TEMED (tetramethylethylenediamine) (Bio-Rad). The membranes were blocked in 5% milk (Marvel) in 1× tris-buffered saline [TBS; tris (3 g/liter), NaCl (8 g/liter), KCl (2 g/liter), and AnalR] supplemented with 0.1% Tween 20 (Sigma). Neutrophils (6.25×10^6 cells per sample) were resuspended in 1× SDS-PAGE sample buffer, sonicated (three times for 10 s each at room temperature), and loaded onto an SDS-PAGE acrylamide gel. The presence and relative quantities of the three class IB PI3K subunits in neutrophils were assessed by Western blotting analysis with noncommercial primary antibodies: rabbit anti-p84 (*21*), sheep anti-p101 (*21*), and rabbit anti-p110γ [Onyx Pharmaceuticals (*21*)]. These antibodies were used in TBS (pH 8.0), supplemented with 0.1% Tween 20 and 4% milk, and were detected with a horseradish peroxidase (HRP)–conjugated goat anti-rabbit antibody for p84 and p110γ (Bio-Rad) or an HRP-conjugated rabbit anti-sheep antibody for p101 (Jackson ImmunoResearch Laboratories) and visualized with ECL reagent (Amersham).

Analysis of the phosphorylation of Akt

Neutrophils (1×10^6 cells per sample) were stimulated with different agonists for different times (as indicated in the figure legends) at 37°C. The sources of agonists were as follows: fMLP (Sigma, no. F3506), C5a (Sigma, no. C5788), LTB_4 (Biomol, Enzo Life Sciences, no. LB-004), and PMA (Sigma, no. P8139). At an appropriate time, the cell suspensions at 37°C were diluted in ice-cold PBS to stop the reaction, centrifuged, and resuspended in 1× SDS-PAGE sample buffer. The samples were then sonicated (three times for 10 s each at room temperature), resolved by SDS-PAGE, and analyzed by Western blotting. Phosphorylation of Akt at Thr^{308} and Ser^{473} was assessed with a mouse anti–Akt-pThr^{308} antibody (Cell Signaling/New England Biolabs) and a rabbit anti–Akt-pSer^{473} antibody (Cell Signaling) in TBS (pH 8.0), 0.1% Tween 20, and 5% BSA. Rabbit antibody against p47^{phox} was used to assess equal loading of lanes on each gel. Membranes were then incubated with LI-COR specific secondary antibodies (Odyssey 800, no. 926-32210, and Odyssey 680, no. 926-32221). The membranes were then scanned by the LI-COR Odyssey membrane scanner and analyzed with Odyssey software version 3.0.1.

PIP_3 and stearoyl/arachidonoyl-DAG assays by mass spectrometry

After purification, neutrophils were resuspended in dPBS (2.50×10^5 cells per sample in a total volume of 153 μl), stimulated with 10 μM fMLP (17 μl of a 100 μM fMLP solution) at 37°C for the times indicated in the legends, and diluted in 750 μl of a 20:10:1 mixture of $CHCl_3$/MeOH/0.01 M HCl. Phosphoinositide internal standards (C16- and C17-PI, -PS, and -PIP_3) were added (100 ng per standard and per sample). The phases were then split by adding 725 μl of $CHCl_3$ (Romil) and 70 μl of 2 M HCl, and the solution was centrifuged for 3 min at 2000*g*. The lower phase was collected and washed with 708 μl of a 3:48:47 mixture of $CHCl_3$/MeOH/0.01 M HCl for 3 min at 2000*g*. The lower phase was then collected, and every trace of aqueous solution was removed with a Gilson 200-μl air pipette. We then added 10 μl of trimethylsilyl-diazomethane (Sigma) to each sample to rapidly and completely methylate the phosphate groups of the inositol ring of the phosphoinositides. After 10 min, glacial acetic acid (6 μl per sample) was added to stop the reaction, and the solution was washed twice with a 3:44:47 mixture of $CHCl_3$/MeOH/H_2O. The lower phase was collected, and 100 μl of 90% MeOH was added before the sample was dried. The drying was performed in a SpeedVac concentrator (Savant) for 45 min at the lowest pressure at room temperature. The lipids were then resuspended in 100 μl of 80% MeOH and analyzed by the lipidomics facility at the Babraham Institute (*33*). Stearoyl/arachidonoyl-DAG was measured as described previously (*17*).

Measurement of free cytoplasmic Ca^{2+} concentrations in mouse neutrophils

We used a flow cytometry–based approach with Fluo3 AM and Fura Red AM to measure the free Ca^{2+} concentration in the cytoplasm of isolated mouse neutrophils in suspension, as described previously (*34*).

In vivo migration assays

Mice were injected intraperitoneally with 0.25 ml of 3% thioglycollate (thioglycollate broth, Sigma) 4.5 hours before culling. Noninjected mice were used as controls. Once the mice were culled, their peritoneums were washed with a solution of PBS, 5 mM EDTA, and the collected cells were counted with a Casy cell counter (Innovatis AG). The cell suspension was labeled with fluorescein isothiocyanate (FITC)–conjugated anti-GR1 (anti–granulocyte receptor 1) antibody (BD Pharmingen) and phycoerythrin-conjugated anti-CD11b antibody (BD Pharmingen) to detect neutrophils with a Fortessa flow cytometer, and the percentages of neutrophils in the cell suspensions were calculated. The total number of peritoneal neutrophils was finally calculated for each mouse and plotted as shown in the figures.

Reconstitution of recipient mice with bone marrow cells

The p84$^{+/+}$, p84$^{-/-}$, p101$^{+/+}$, and p101$^{-/-}$ recipient mice were subjected to γ-irradiation 24 hours before the injection process with two doses of 5 Gy, which were separated by 3 hours. The p84$^{+/+}$, p84$^{-/-}$, p101$^{+/+}$, and p101$^{-/-}$ donor mice were culled, and their bone marrow was collected with a 21-gauge needle into PBS, 10% fetal bovine serum (Bioclear) and filtered through a 40-μm cell strainer (BD Falcon). Once resuspended at a concentration of 5×10^7 cells/ml, 100 μl of the bone marrow suspension was injected intravenously in the tail veins of the selected recipient mice with a 21-gauge needle. The injected mice then received drinking water containing neomycin at a final concentration of 2 mg/ml for 2 weeks to minimize their chances of becoming infected during the critical period of reconstitution.

Transwell assays

Bone marrow cells were collected into Transwell assay buffer [TAB: HBSS with Ca^{2+} and Mg^{2+} (Sigma) containing 0.25% fatty acid–free, low-endotoxin BSA and 14 mM Hepes–NaOH (pH 7.2)] at 37°C at a concentration of 5×10^6 cells/ml. These cell suspensions (200 μl) were added to the top of a Transwell filter insert (polycarbonate, 3-μm pore; Millipore) inserted into a 24-well plate (Ultra-Low Attachment; Costar, Corning) containing 300 μl of TAB containing fMLP or vehicle. The plates were then transferred to an incubator (37°C, atmospheric CO_2, humidified). After 1 hour, the filter inserts were discarded, and the medium in the lower chamber was removed, retained, and replaced by 300 μl of Wash Buffer containing 5 mM EDTA. After 30 min on ice, the buffer in each of the wells was removed and pooled. A further 300 μl of Wash Buffer was rinsed through the wells and added to the pools, which were made up to 1 ml with Wash Buffer. The cells recovered from each of the wells were analyzed by flow cytometry, counting neutrophils through a gate defined by Gr1$^+$ cells in the total bone marrow. The total bone marrow preparation was stained for Gr1 (after incubation in Fc block) with FITC-conjugated anti-GR1 antibody (0.125 mg/ml) before being washed and analyzed by flow cytometry. This analysis

was used to define a gate through which the number of neutrophils that went into each upper chamber could be estimated and to quantify the number of neutrophils that had migrated into the lower chamber.

In vitro chemotaxis EZ-TAXIS assays

To measure chemotaxis, we used the EZ-TAXIS chamber (*35*). Briefly, the chamber is composed of a silicon chip clamped to a fibrinogen-coated glass coverslip (Sigma, no. F8630) to form six compartments. Each of these compartments has two wells into which the cells and agonists are added. These wells are separated by a 300-μm long and 5-μm high bridge on which the cells migrate. After filling the chamber with Migration Buffer ($dPBS^{++}$ supplemented with 0.1% fatty acid–free BSA and 15 mM Hepes) and eliminating the air bubbles inside the unit, 2 μl of the cell suspension (3×10^5 cells/ml) was added on one side of the bridge. To align the cells against the bridge, 7 μl of buffer was removed from the agonist side well. Once set, 1 μl of 30 μM fMLP was added to the agonist well with a PB-600 repeating dispenser equipped with a 25 μl Hamilton syringe.

Measurement of F-actin polymerization

Mouse neutrophils were isolated at 4°C, suspended at 5×10^6 cells/ml in Migration Buffer, and equilibrated for 2 min at 37°C. Per sample, 1×10^6 cells were stimulated, for the indicated periods, with 10 μM fMLP and then were fixed in an equal volume of 4% paraformaldehyde (to give a final concentration of 2%) for 15 min at room temperature. Fixed cells were diluted in an excess volume of Migration Buffer and centrifuged at 500*g* for 4 min at room temperature, after which the supernatants were discarded. Cells were resuspended in 1 ml of Migration Buffer and recentrifuged. Supernatants were discarded, and cells were resuspended in 200 μl of staining buffer [Migration Buffer containing 1% Triton X-100 and TRITC-phalloidin (50 ng/ml, Sigma)] and incubated for 15 min at room temperature. Cells were then washed twice in Migration Buffer, suspended in 200 μl of Migration Buffer, and imaged under wide-field epifluorescence with an Olympus CellR microscope and a 60× objective.

Analysis of ROS production

After purification, neutrophils were resuspended in $dPBS^{++}$ supplemented with 0.03% $NaHCO_3$ and 0.1% glucose at 6.25×10^6 cells/ml and incubated with 300 μM luminol (Sigma) and HRP (55 U/ml, Sigma) for 5 min at 37°C. Cells were then added to a prewarmed, polystyrene 96-well plate (Berthold Technologies) that contained varying concentrations of agonists (as described in the figure legends), and measurement was started immediately. Light emission was recorded by a Berthold Microlumat Plus luminometer (Berthold Technologies).

Statistical analysis

The tests of statistical significance we applied are defined in the figure legends.

SUPPLEMENTARY MATERIALS

www.sciencesignaling.org/cgi/content/full/8/360/ra8/DC1

Fig. S1. Targeting of *PIK3R6* and analysis of blood cell counts for $p84^{-/-}$ mice.

Fig. S2. Ca^{2+} and stearoyl/arachidonoyl-DAG signaling in mouse neutrophils.

Table S1. Primers used to generate probes for Southern blotting and for genotyping the different mouse strains.

REFERENCES AND NOTES

1. B. Vanhaesebroeck, L. Stephens, P. Hawkins, PI3K signalling: The path to discovery and understanding. *Nat. Rev. Mol. Cell Biol.* **13**, 195–203 (2012).
2. C. Costa, E. L. Martin-Conte, E. Hirsch, Phosphoinositide 3-kinase p110γ in immunity. *IUBMB Life* **63**, 707–713 (2011).
3. E. Hirsch, V. L. Katanaev, C. Garlanda, O. Azzolino, L. Pirola, L. Silengo, S. Sozzani, A. Mantovani, F. Altruda, M. P. Wymann, Central role for G protein–coupled phosphoinositide 3-kinase γ in inflammation. *Science* **287**, 1049–1053 (2000).
4. Z. Li, H. Jiang, W. Xie, Z. Zhang, A. V. Smrcka, D. Wu, Roles of PLC-β2 and -β3 and PI3Kγ in chemoattractant-mediated signal transduction. *Science* **287**, 1046–1049 (2000).
5. T. Sasaki, J. Irie-Sasaki, R. G. Jones, A. J. Oliveira-dos-Santos, W. L. Stanford, B. Bolon, A. Wakeham, A. Itie, D. Bouchard, I. Kozieradzki, N. Joza, T. W. Mak, P. S. Ohashi, A. Suzuki, J. M. Penninger, Function of PI3Kγ in thymocyte development, T cell activation, and neutrophil migration. *Science* **287**, 1040–1046 (2000).
6. G. J. Ferguson, L. Milne, S. Kulkarni, T. Sasaki, S. Walker, S. Andrews, T. Crabbe, P. Finan, G. Jones, S. Jackson, M. Camps, C. Rommel, M. Wymann, E. Hirsch, P. Hawkins, L. Stephens, PI(3)Kγ has an important context-dependent role in neutrophil chemokinesis. *Nat. Cell Biol.* **9**, 86–91 (2007).
7. M. Camps, T. Rückle, H. Ji, V. Ardissone, F. Rintelen, J. Shaw, C. Ferrandi, C. Chabert, C. Gillieron, B. Françon, T. Martin, D. Gretener, D. Perrin, D. Leroy, P. A. Vitte, E. Hirsch, M. P. Wymann, R. Cirillo, M. K. Schwarz, C. Rommel, Blockade of PI3Kγ suppresses joint inflammation and damage in mouse models of rheumatoid arthritis. *Nat. Med.* **11**, 936–943 (2005).
8. S. Suire, J. Coadwell, G. J. Ferguson, K. Davidson, P. Hawkins, L. Stephens, p84, a new Gβγ-activated regulatory subunit of the type IB phosphoinositide 3-kinase p110γ. *Curr. Biol.* **15**, 566–570 (2005).
9. P. Voigt, M. B. Dorner, M. Schaefer, Characterization of $p87^{PIKAP}$, a novel regulatory subunit of phosphoinositide 3-kinase γ that is highly expressed in heart and interacts with PDE3B. *J. Biol. Chem.* **281**, 9977–9986 (2006).
10. B. Stoyanov, S. Volinia, T. Hanck, I. Rubio, M. Loubtchenkov, D. Malek, S. Stoyanova, B. Vanhaesebroeck, R. Dhand, B. Nürnberg, P. Gierschik, K. Seedorf, J. Justin Hsuan, M. D. Waterfield, R. Wetzker, Cloning and characterization of a G protein–activated human phosphoinositide-3 kinase. *Science* **269**, 690–693 (1995).
11. U. Maier, A. Babich, B. Nürnberg, Roles of non-catalytic subunits in Gβγ-induced activation of class I phosphoinositide 3-kinase isoforms β and γ. *J. Biol. Chem.* **274**, 29311–29317 (1999).
12. L. R. Stephens, A. Eguinoa, H. Erdjument-Bromage, M. Lui, F. Cooke, J. Coadwell, A. S. Smrcka, M. Thelen, K. Cadwallader, P. Tempst, P. T. Hawkins, The Gβγ sensitivity of a PI3K is dependent upon a tightly associated adaptor, p101. *Cell* **89**, 105–114 (1997).
13. O. Vadas, H. A. Dbouk, A. Shymanets, O. Perisic, J. E. Burke, W. F. Abi Saab, B. D. Khalil, C. Harteneck, A. R. Bresnick, B. Nürnberg, J. M. Backer, R. L. Williams, Molecular determinants of PI3Kγ-mediated activation downstream of G-protein–coupled receptors (GPCRs). *Proc. Natl. Acad. Sci. U.S.A.* **110**, 18862–18867 (2013).
14. B. Kurig, A. Shymanets, T. Bohnacker, Prajwal, C. Brock, M. R. Ahmadian, M. Schaefer, A. Gohla, C. Harteneck, M. P. Wymann, E. Jeanclos, B. Nürnberg, Ras is an indispensable coregulator of the class I_B phosphoinositide 3-kinase p87/p110γ. *Proc. Natl. Acad. Sci. U.S.A.* **106**, 20312–20317 (2009).
15. P. Rodriguez-Viciana, P. H. Warne, R. Dhand, B. Vanhaesebroeck, I. Gout, M. J. Fry, M. D. Waterfield, J. Downward, Phosphatidylinositol-3-OH kinase as a direct target of Ras. *Nature* **370**, 527–532 (1994).
16. M. E. Pacold, S. Suire, O. Perisic, S. Lara-Gonzalez, C. T. Davis, E. H. Walker, P. T. Hawkins, L. Stephens, J. F. Eccleston, R. L. Williams, Crystal structure and functional analysis of Ras binding to its effector phosphoinositide 3-kinase γ. *Cell* **103**, 931–943 (2000).
17. S. Suire, C. Lécureuil, K. E. Anderson, G. Damoulakis, I. Niewczas, K. Davidson, H. Guillou, D. Pan, J. Clark, P. T. Hawkins, L. Stephens, GPCR activation of Ras and PI3Kγ in neutrophils depends on PLCβ2/β3 and the RasGEF RasGRP4. *EMBO J.* **31**, 3118–3129 (2012).
18. R. Walser, J. E. Burke, E. Gogvadze, T. Bohnacker, X. Zhang, D. Hess, P. Küenzi, M. Leitges, E. Hirsch, R. L. Williams, M. Laffargue, M. P. Wymann, PKCβ phosphorylates PI3Kγ to activate it and release it from GPCR control. *PLOS Biol.* **11**, e1001587 (2013).
19. L. Stephens, A. Eguinoa, S. Corey, T. Jackson, P. T. Hawkins, Receptor stimulated accumulation of phosphatidylinositol (3,4,5)-trisphosphate by G-protein mediated pathways in human myeloid derived cells. *EMBO J.* **12**, 2265–2273 (1993).
20. A. E. Traynor-Kaplan, B. L. Thompson, A. L. Harris, P. Taylor, G. M. Omann, L. A. Sklar, Transient increase in phosphatidylinositol 3,4-bisphosphate and phosphatidylinositol trisphosphate during activation of human neutrophils. *J. Biol. Chem.* **264**, 15668–15673 (1989).
21. S. Suire, A. M. Condliffe, G. J. Ferguson, C. D. Ellson, H. Guillou, K. Davidson, H. Welch, J. Coadwell, M. Turner, E. R. Chilvers, P. T. Hawkins, L. Stephens, Gβγs and the Ras binding domain of p110γ are both important regulators of PI3Kγ signalling in neutrophils. *Nat. Cell Biol.* **8**, 1303–1309 (2006).
22. A. M. Condliffe, K. Davidson, K. E. Anderson, C. D. Ellson, T. Crabbe, K. Okkenhaug, B. Vanhaesebroeck, M. Turner, L. Webb, M. P. Wymann, E. Hirsch, T. Ruckle, M. Camps, C. Rommel, S. P. Jackson, E. R. Chilvers, L. R. Stephens, P. T. Hawkins, Sequential activation of class IB and class IA PI3K is important for the primed respiratory burst of human but not murine neutrophils. *Blood* **106**, 1432–1440 (2005).
23. M. J. Wakelam, Diacylglycerol—When is it an intracellular messenger? *Biochim. Biophys. Acta* **1436**, 117–126 (1998).

24. K. D. Puri, T. A. Doggett, C. Y. Huang, J. Douangpanya, J. S. Hayflick, M. Turner, J. Penninger, T. G. Diacovo, The role of endothelial PI3Kγ activity in neutrophil trafficking. *Blood* **106**, 150–157 (2005).
25. M. Nishio, K. Watanabe, J. Sasaki, C. Taya, S. Takasuga, R. Iizuka, T. Balla, M. Yamazaki, H. Watanabe, R. Itoh, S. Kuroda, Y. Horie, I. Förster, T. W. Mak, H. Yonekawa, J. M. Penninger, Y. Kanaho, A. Suzuki, T. Sasaki, Control of cell polarity and motility by the PtdIns(3,4,5)P_3 phosphatase SHIP1. *Nat. Cell Biol.* **9**, 36–44 (2007).
26. T. Bohnacker, R. Marone, E. Collmann, R. Calvez, E. Hirsch, M. P. Wymann, PI3Kγ adaptor subunits define coupling to degranulation and cell motility by distinct PtdIns(3,4,5)P_3 pools in mast cells. *Sci. Signal.* **2**, ra27 (2009).
27. E. Patrucco, A. Notte, L. Barberis, G. Selvetella, A. Maffei, M. Brancaccio, S. Marengo, G. Russo, O. Azzolino, S. D. Rybalkin, L. Silengo, F. Altruda, R. Wetzker, M. P. Wymann, G. Lembo, E. Hirsch, PI3Kγ modulates the cardiac response to chronic pressure overload by distinct kinase-dependent and -independent effects. *Cell* **118**, 375–387 (2004).
28. J. A. Brazzatti, M. Klingler-Hoffmann, S. Haylock-Jacobs, Y. Harata-Lee, M. Niu, M. D. Higgins, M. Kochetkova, P. Hoffmann, S. R. McColl, Differential roles for the p101 and p84 regulatory subunits of PI3Kγ in tumor growth and metastasis. *Oncogene* **31**, 2350–2361 (2012).
29. G. Damoulakis, L. Gambardella, K. L. Rossman, C. D. Lawson, K. E. Anderson, Y. Fukui, H. C. Welch, C. J. Der, L. R. Stephens, P. T. Hawkins, P-Rex1 directly activates RhoG to regulate GPCR-driven Rac signalling and actin polarity in neutrophils. *J. Cell Sci.* **127**, 2589–2600 (2014).
30. I. A. Prior, J. F. Hancock, Ras trafficking, localization and compartmentalized signalling. *Semin. Cell Dev. Biol.* **23**, 145–153 (2012).
31. W. C. Skarnes, B. Rosen, A. P. West, M. Koutsourakis, W. Bushell, V. Iyer, A. O. Mujica, M. Thomas, J. Harrow, T. Cox, D. Jackson, J. Severin, P. Biggs, J. Fu, M. Nefedov, P. J. de Jong, A. F. Stewart, A. Bradley, A conditional knockout resource for the genome-wide study of mouse gene function. *Nature* **474**, 337–342 (2011).
32. M. Bunting, K. E. Bernstein, J. M. Greer, M. R. Capecchi, K. R. Thomas, Targeting genes for self-excision in the germ line. *Genes Dev.* **13**, 1524–1528 (1999).
33. J. Clark, K. E. Anderson, V. Juvin, T. S. Smith, F. Karpe, M. J. Wakelam, L. R. Stephens, P. T. Hawkins, Quantification of PtdInsP_3 molecular species in cells and tissues by mass spectrometry. *Nat. Methods* **8**, 267–272 (2011).
34. S. Partida-Sánchez, D. A. Cockayne, S. Monard, E. L. Jacobson, N. Oppenheimer, B. Garvy, K. Kusser, S. Goodrich, M. Howard, A. Harmsen, T. D. Randall, F. E. Lund, Cyclic ADP-ribose production by CD38 regulates intracellular calcium release, extracellular calcium influx and chemotaxis in neutrophils and is required for bacterial clearance in vivo. *Nat. Med.* **7**, 1209–1216 (2001).
35. S. Kanegasaki, Y. Nomura, N. Nitta, S. Akiyama, T. Tamatani, Y. Goshoh, T. Yoshida, T. Sato, Y. Kikuchi, A novel optical assay system for the quantitative measurement of chemotaxis. *J. Immunol. Methods* **282**, 1–11 (2003).

Acknowledgments: We thank Q. Zhang, manager of the lipidomics facility at the Babraham Institute, for measuring phosphoinositides, and J. Clark of the Babraham Institute for measuring stearoyl/arachidonoyl-DAG. We also thank A. Segonds-Pichon of the Babraham Institute for advice on statistical analysis. **Funding:** This work was funded by the UK Biotechnology and Biological Sciences Research Council (grant BB/J004456/1) and the Medical Research Council (grant MR/K018167/1). **Author contributions:** A.D., L.G. (mouse reconstitution), D.P. (mouse reconstitution), and K.E.A. (DAG measurements) performed experiments, and A.D., P.T.H., and L.R.S. planned the work, designed experiments, and wrote the manuscript. **Competing interests:** The authors declare that they have no competing interests.

Submitted 4 June 2014
Accepted 12 December 2014
Final Publication 20 January 2015
10.1126/scisignal.2005564
Citation: A. Deladeriere, L. Gambardella, D. Pan, K. E. Anderson, P. T. Hawkins, L. R. Stephens, The regulatory subunits of PI3Kγ control distinct neutrophil responses. *Sci. Signal.* **8**, ra8 (2015).

The regulatory subunits of PI3Kγ control distinct neutrophil responses

Arnaud Deladeriere, Laure Gambardella, Dingxin Pan, Karen E. Anderson, Phillip T. Hawkins and Len R. Stephens (January 20, 2015)

Science Signaling **8** (360), ra8. [doi: 10.1126/scisignal.2005564]